Structure

Article

Assessing the Structures and Interactions of γD-Crystallin Deamidation Variants

Graphical Abstract

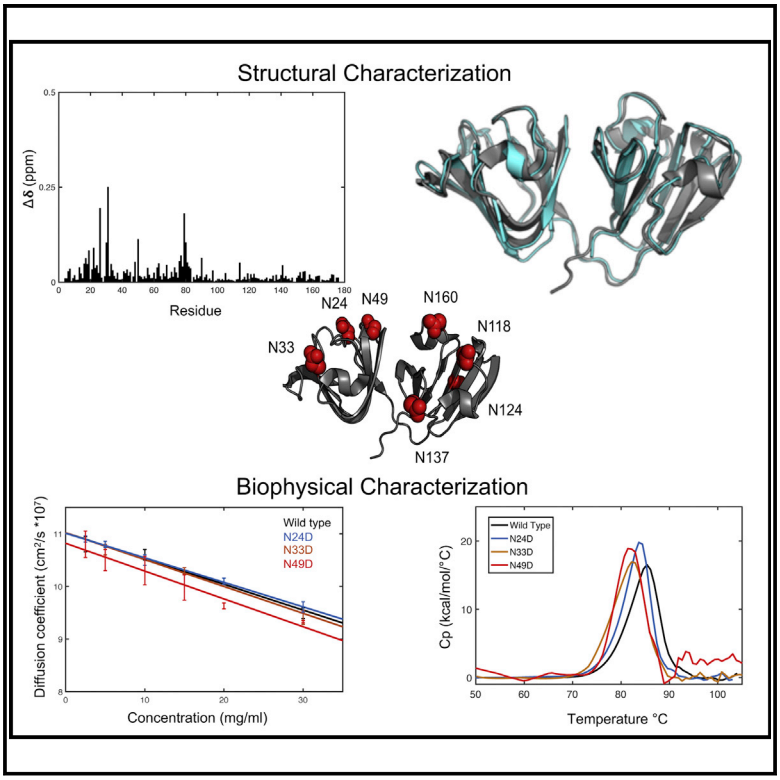

Highlights

- NMR data reveal minimal effects of N deamidation on γD-crystallin structure
- Crystal structures of N124D and N160D are consistent with NMR results
- Deamidation does not alter the colloidal or thermodynamic stability of γD-crystallin

Authors

Alex J. Guseman, Matthew J. Whitley, Jeremy J. González, Nityam Rathi, Mikayla Ambarian, Angela M. Gronenborn

Correspondence

amg100@pitt.edu

In Brief

Guseman et al. combined NMR, X-ray crystallography, dynamic light scattering, and DSC to demonstrate that single Asn to Asp deamidation has minimal influence on the properties and structure of γD-crystallin.

Guseman et al., 2021, Structure *29*, 1–8
March 4, 2021
https://doi.org/10.1016/j.str.2020.11.006

CellPress

Please cite this article in press as: Guseman et al., Assessing the Structures and Interactions of γD-Crystallin Deamidation Variants, Structure (2020), https://doi.org/10.1016/j.str.2020.11.006

Structure

CellPress

Article

Assessing the Structures and Interactions of γD-Crystallin Deamidation Variants

Alex J. Guseman,[1] Matthew J. Whitley,[1,2] Jeremy J. González,[1] Nityam Rathi,[1] Mikayla Ambarian,[1] and Angela M. Gronenborn[1,3,*]

[1]Department of Structural Biology, University of Pittsburgh School of Medicine, 3501 Fifth Avenue, Pittsburgh, PA 15261, USA
[2]Present address: Department of Pharmacology and Chemical Biology, University of Pittsburgh School of Medicine, Pittsburgh, PA 15261, USA
[3]Lead Contact
*Correspondence: amg100@pitt.edu
https://doi.org/10.1016/j.str.2020.11.006

SUMMARY

Cataracts involve the deposition of the crystallin proteins in the vertebrate eye lens, causing opacification and blindness. They are associated with either genetic mutation or protein damage that accumulates over the lifetime of the organism. Deamidation of Asn residues in several different crystallins has been observed and is frequently invoked as a cause of cataract. Here, we investigated the properties of Asp variants, deamidation products of γD-crystallin, by solution NMR, X-ray crystallography, and other biophysical techniques. No substantive structural or stability changes were noted for all seven Asn to Asp γD-crystallins. Importantly, no changes in diffusion interaction behavior could be detected. Our combined experimental results demonstrate that introduction of single Asp residues on the surface of γD-crystallin by deamidation is unlikely to be the driver of cataract formation in the eye lens.

INTRODUCTION

Over 20 million people are affected by cataracts, the leading cause of blindness worldwide (Lam et al., 2015). Cataract denotes an opacification of the eye lens, brought about by insoluble aggregates of crystallin proteins. The eye lens is a highly unique and specialized organ in the human body, evolved to focus light onto the retina and, at the same time, minimize any scattering of the incoming light (Bloemendal et al., 2004; Zhao et al., 2011a, 2011b). This is achieved by a uniform distribution of the crystallin proteins at concentrations exceeding 400 g/L, as well as an absence of organelles and large protein machineries in mature lens cells. In essence, a developed lens cell can be viewed as a transparent, densely packed sack of crystallin proteins (Bloemendal et al., 2004; Lam et al., 2015; Sharma and Santhoshkumar, 2009). Since mature lens cells are devoid of protein machines and processes that are necessary for protein synthesis and degradation, essentially no protein turnover takes place. As a result, crystallins are required to be stable and functional over an organism's entire lifespan. They are prototypical members of so-called long-lived proteins (Toyama and Hetzer, 2012; Lynnerup et al., 2008). If damage or other insults compromise their integrity and solubility, aggregation and cataract formation may ensue.

Crystallins are divided into three subfamilies: α-, β-, and γ-crystallins. α-Crystallins are large, polydisperse oligomers that resemble heat shock proteins (Jehle et al., 2010) and are thought to serve as chaperones that help to keep β/γ-crystallins functional (Ghosh and Chauhan, 2019; Haslbeck et al., 2016). β/γ-Crystallins are small, extremely stable, and soluble proteins, functioning predominantly to safeguard the optical properties of the eye lens. All β/γ-crystallins have evolved from a common ancestor, exhibiting homologous amino acid sequences that adopt similar secondary and tertiary structures (Bloemendal et al., 2004; Jaenicke and Slingsby, 2001). They are made up of two domains, each containing two unique antiparallel β sheet arrangements, known as Greek keys (Basak et al., 2003; Bloemendal et al., 2004). While γ-crystallins are monomeric, β-crystallins can be dimeric or oligomeric (Jaenicke and Slingsby, 2001).

Despite their high stability and the presence of α-crystallin chaperones, the integrity of the crystallins in the eye lens can become compromised with age. In fact, different types of stress, such as exposure to UV radiation, oxidative stress, and other insults can result in chemical modifications of the lens proteins, including deamidation, glycation, altered disulfide bond formation, and peptide bond cleavage (Sharma and Santhoshkumar, 2009; Hanson et al., 2000; Wilmarth et al., 2006; Serebryany et al., 2018). A leading hypothesis for age-related cataract invokes the accumulation of damaged crystallin proteins, which, in turn, irreversibly aggregate to form insoluble precipitates (Warmack et al., 2019). Proteomic analysis has shown the presence of modified crystallins in aged lenses, and γ-crystallin deamidation has been implicated as a potential driver of cataract

Please cite this article in press as: Guseman et al., Assessing the Structures and Interactions of γD-Crystallin Deamidation Variants, Structure (2020), https://doi.org/10.1016/j.str.2020.11.006

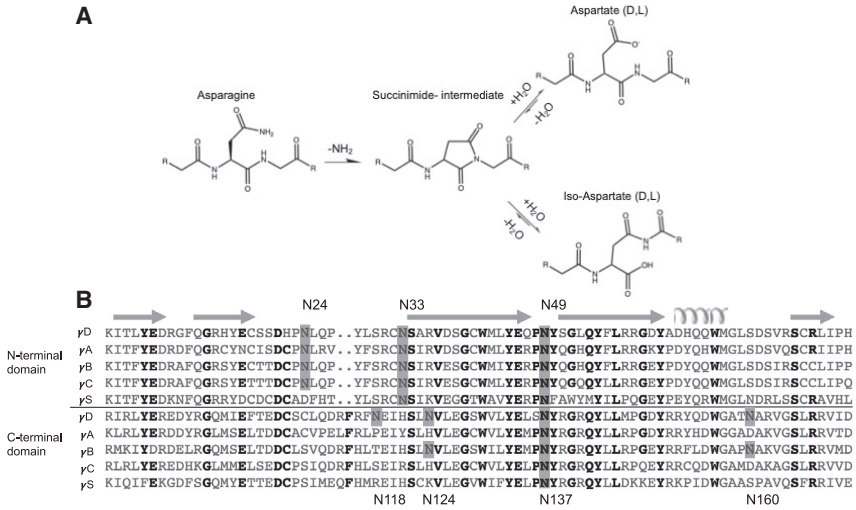

Figure 1. Deamidation and Asparagines in γD-Crystallin

(A) Deamidation pathway of asparagine residues.

(B) Amino acid sequence alignment of γ-crystallins. Three of the seven Asn residues are strictly conserved.

formation (Sharma and Santhoshkumar, 2009; Hains and Truscott, 2010; Lampi et al., 2014).

Deamidation is a stochastic chemical process that converts glutamine (Gln) and asparagine (Asn) residues to glutamate or iso-glutamate and aspartate (Asp) or iso-Asp, respectively (Clarke, 1987; Geiger and Clarke, 1987). At neutral pH, Asn deamidation is more common than Gln deamidation and proceeds primarily via a succinimide intermediate, a short-lived ring structure that is formed between the carboxyl side chain and the amide group of the following amino acid in the sequence (Figure 1A). The succinimide ring undergoes hydrolysis, resolving into either aspartate or iso-aspartate. Rates of deamidation of individual amide residues depend upon primary sequence, three-dimensional structure, and solution properties, such as pH, temperature, ionic strength, and buffer ions (Robinson, 2002; Warmack et al., 2019). Both deamidation products of Asn reduce the protein's net charge by 1 unit, and, in the case of iso-aspartate, an additional methylene group becomes inserted into the protein backbone following the Cα, thereby causing a distortion in the native connection between peptide planes. In the majority of somatic cells, deamidation is of minimal overall significance since it is a relatively slow kinetic process and normal protein turnover ensures that deamidated proteins are removed and replaced by newly synthesized ones. However, because there is no protein turnover in differentiated lens cells, even a stochastic and kinetically slow process like deamidation can, over time, result in the accumulation of modified crystallins with potentially grave consequences (Toyama and Hetzer, 2012).

Here, we report an investigation of whether and how the deamidation of Asn to Asp influences crystallin behavior and structure. We chose to evaluate human γD-crystallin since it is the third most abundant γ-crystallin in the lens. Specifically, γD-crystallin represents ~7% of the crystallin protein mass (Lampi et al., 1998; Robinson et al., 2006) and is a major component of the lens nucleus, the oldest part of the lens (Ji et al., 2013a; Bloemendal et al., 2004). Our group has studied human γD-crystallin extensively (Boatz et al., 2017; Ji et al., 2012, 2013a, 2013b; Whitley et al., 2017), and, in this study, we changed each of its seven Asn residues to Asp and characterized these deamidation variants by nuclear magnetic resonance (NMR), differential scanning calorimetry (DSC), dynamic light scattering (DLS), and X-ray crystallography. Surprisingly, no substantive stability or structural changes were noted in any of the variants, and no changes in diffusion interaction behavior could be detected.

RESULTS

Each of the seven Asn residues in human γD-crystallin (Figure 1B) were mutated to Asp and the proteins were structurally characterized. To this end, ^{1}H-^{15}N HSQC spectra were recorded and used as a "fingerprint" of the proteins' three-dimensional structures (Forman-Kay et al., 1992). As demonstrated from the differences in amide chemical shifts for all the mutants, compared with wild-type γD-crystallin (Figure 2), no large differences (>0.5 ppm) are noted for any variant, apart from N33D. Small deviations from the wild-type resonance frequencies are noted for amino acids close to the mutation site and, in general, these changes are restricted to the domains that harbor the mutation site. Thus, for N24D, N33D, and N49D, essentially no chemical shift changes are observed for any residues in the C-terminal domain (CTD). Likewise, for the N118D, N124D, N137D, and N160D variants that possess mutations in the CTD, no substantive chemical shift changes are seen for amide resonances of amino acids in the N-terminal domain (NTD). Interestingly, for N33D, we observed non-negligible chemical shift changes throughout the NTD, with 11 amide resonances exhibiting differences of 0.2–1.15 ppm, compared with their wild-type counterparts. The largest shift differences are associated with residues R32 and S34, which experience amide proton shift differences of −0.022 and 0.23 ppm, respectively, and ^{15}N shift differences of −1.30 and 2.78 ppm, respectively (Figure S1). N33 is the first amino acid in β strand 3 of the NTD and participates in a hydrogen bonding network involving Y6 in β strand 1 across the β sheet structure of the Greek key motif. Two further H bonds are present between the side-chain amino group of N33 and the backbone carboxyl of E7 and the D73 side chain in the loop following the short α helix. Therefore, the effect of the N33D mutation could easily propagate to the neighboring structural elements via this hydrogen bonding network. Indeed, the importance of the conserved sequence signature of Y6, E7, F11, G13, and S34 of motif 1 in the arrangement of the first Greek key in the crystallin domain fold has been emphasized previously (Jaenicke and Slingsby, 2001).

In addition to using NMR for characterizing the structural changes induced by the Asn to Asp mutation, we also used crystallography. Although crystallization trials were carried out for all the deamidation variants, diffraction quality crystals were obtained for only two, N124D and N160D, up to now. Their crystal structures were solved to 1.15 and 1.2 Å, respectively (Table 1).

Please cite this article in press as: Guseman et al., Assessing the Structures and Interactions of γD-Crystallin Deamidation Variants, Structure (2020), https://doi.org/10.1016/j.str.2020.11.006

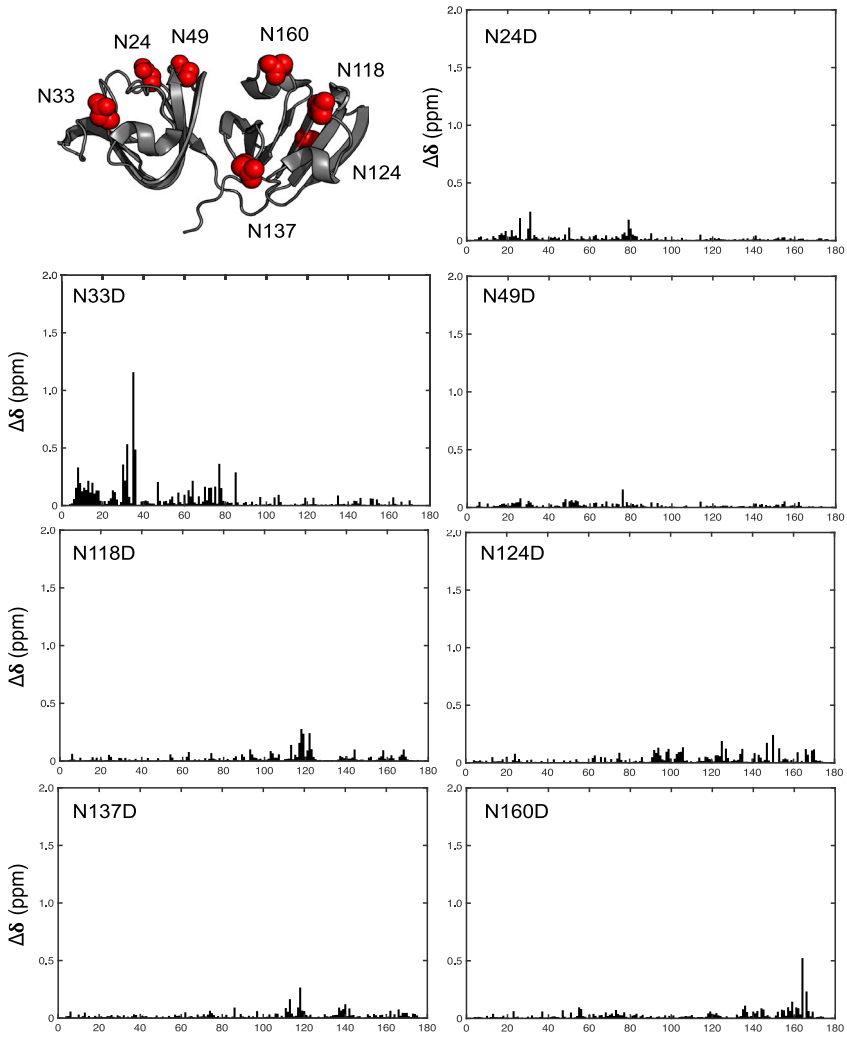

Figure 2. NMR Chemical Shift Changes in Deamidated γD-Crystallin Variants

Overall structure of wild-type γD-crystallin in ribbon representation with all asparagine side chains depicted in red space filling representation (top left) and amide chemical shift changes of deamidation variants, relative to wild-type γD-crystallin. Only small changes are observed, except for N33D, which exhibits larger changes close to the mutation site.

The crystal structures confirmed the NMR findings that only very small conformational changes are present in these two variants: superposition of the NTD (residues 1–81) and CTD (residues 89–17) of the N124D mutant (cyan, Figure 3, left) onto those of wild-type γD-crystallin (gray, Figure 4, left) yielded average pairwise backbone root-mean-square deviation (RMSD) values of 0.279 and 0.182 Å, respectively. For the N160D mutant (green, Figure 3, right), average pairwise backbone RMSD values of 0.300 and 0.219 Å, are seen for the NTD and CTD coordinates, respectively. As an aside, the two molecules of N160D in the asymmetric unit exhibit an average pairwise backbone RMSD value of 0.269 Å, validating that the structures are essentially identical.

We further investigated whether any of the Asn to Asp mutants exhibited significantly reduced thermodynamic stability compared with wild-type γD-crystallin. To this end, DSC was used. Unfortunately, all the mutant crystallins, as well as the wild-type protein, displayed visible precipitation upon thermal unfolding, which precluded the extraction of accurate thermodynamic parameters. However, the thermograms (Figure S2) still yielded reliable values for the melting temperature. For all the investigated crystallins, the apparent T_m values range from 80°C to 85°C, with a T_m of 81.2°C for wild-type (Table 2). Only one mutant, N137D, exhibited a lower melting temperature than wild-type γD-crystallin; all others were higher, with N160D being the highest. All T_m values are within 3.1°C of the average value of 82.4°C, just twice the standard deviation (±1.61°C).

In addition to thermal stability, reversible association in solution, also called colloidal stability, was evaluated by measuring the diffusivity, or diffusion interaction parameter (DIP) of the different Asn to Asp mutants by DLS. This parameter is dominated by weak, attractive forces related to surface charges. Since each individual Asn to Asp change alters the charge in seven different locations on the γD-crystallin surface, the DIP represents an ideal measure for effects imparted by charge-mediated association. Wild-type γD-crystallin and all Asn to Asp mutants yielded DIP values of similar magnitude, between −3 and −6 mL/g (Figure 4; Table 3). All values lie within the error range of the value for wild-type γD-crystallin, namely −4 ± 1 mL/g. Thus, no significant changes in weak associative interactions for the different variants in solution were detected over a 10-fold change in protein concentration, ranging from 2.5 to 30 mg/mL.

Since the interaction between proteins is governed by the respective protein surfaces, we calculated the solvent accessible surface area (SASA) for all heavy atoms of the seven Asn residues in the solution NMR structure (PDB: 2KLJ; Wang et al., 2009) using the protSA server (Estrada et al., 2009) for assessing the potential impact of Asp mutations. All Asn residues are located on the surface of the protein (Figure 2, top left) and are largely solvent exposed, with the exceptions of N33 and N124 where only the amino or carbonyl side-chain groups are accessible to solvent (Figure S3). Uniquely, N33 was the least solvent exposed with just the side-chain carboxyl oxygen (OD1) of N33 possessing 5 $Å^2$ of SASA.

DISCUSSION

Deamidation of Asn residues is a common modification found in long-lived proteins and is often invoked as a cause for age-related

Please cite this article in press as: Guseman et al., Assessing the Structures and Interactions of γD-Crystallin Deamidation Variants, Structure (2020), https://doi.org/10.1016/j.str.2020.11.006

Table 1. X-Ray Data Collection and Refinement Statistics

	N124D γ D-Crystallin	N160D γ D-Crystallin
PDB:	6W5B	6WCY
Data Collection		
Wavelength (Å)	0.8856	1.0
Space group	$P2_12_12_1$	$P2_12_12_1$
Unit cell dimensions		
α, β, γ (Å)	33.65, 51.49, 93.79	50.81, 51.87, 113.99
a, b, c (°)	90, 90, 90	90, 90, 90
No. of unique reflections	58,473	85,435
Multiplicity	11.6	12.9
Completeness (%)	99.3 (93.9)	90.9 (52.5)
Mean I/σ(I)	17.4 (2.2)	22.50 (1.0)
Wilson B factor	12.4	17.3
R_{merg}	0.068 (0.519)	0.053 (1.185)
R_{meas}	0.071 (0.575)	0.055 (1.324)
R_{pim}	0.020 (0.241)	0.015 (0.568)
CC½	0.999 (0.963)	0.999 (0.450)
Refinement		
Resolution range (Å)	28.17–1.15	34.59–1.20
Molecules per ASU	1	2
R_{work}, R_{free}	0.151, 0.173	0.169, 0.195
CC_{work}, CC_{free}	0.963, 0.959	0.971, 0.967
No. of non-H atoms		
Macromolecules	1,482	2,911
Water	193	351
RMSD		
Bonds (Å)	0.011	0.009
Angles (°)	1.48	1.21
Ramachandran plot (%)		
Favored	98.21	99.41
Allowed	1.79	0.29
Outliers	0.0	0.29
Average B factor		
Macromolecules	16.6	21.7
Water	28.4	31.4

Values in parentheses refer to the highest-resolution shell. The set of free reflections for R_{free} and CC_{free} were calculated with 5% of the total reflections, and these reflections were not included in the model building and refinement process.
RMSD, root-mean-square deviation.

cataracts (Hains and Truscott, 2010; Hanson et al., 2000; Lampi et al., 2001, 2012, 2014, 2016; Michiel et al., 2010; Srivastava and Srivastava, 2003; Warmack et al., 2019). Since structure and stability are key attributes for safeguarding function, we performed a comprehensive study of the seven possible end products of γD-crystallin deamidation. Both NMR and crystallographic characterizations of the seven Asn to Asp mutants revealed minimal structural perturbations. Only N33D exhibited local chemical shift changes (Figure S4). Although initially surprising, our findings may be explained by an analysis of the γ-crystallin protein family sequences and the specific locations of the implicated residues in the protein structure. Alignment of the protein sequences of the five γ-crystallin paralogs shows that only three of the seven Asn residues (N33, N49, and N137) are strictly conserved (Figure 1B). N24 and N160 of γD-crystallin are D24 (in γS-crystallin) and D160 (in γA-crystallin and γC-crystallin). This suggests that, at positions 24 and 160, Asp residues are tolerable, even if the neighboring amino acids are not completely identical to those in γD-crystallin. As a consequence, no gross structural changes would be expected. This notion is consistent with our finding that only N33D, one of the conserved Asn residues, exhibited significant chemical shift changes in the ^{1}H-^{15}N HSQC spectrum.

Why only the N33D mutant exhibited notable ^{1}H,^{15}N amide chemical shift changes can be explained by our SASA data and the H bond networks inferred from the X-ray structures. Our SASA analysis revealed that N33 is buried (Figure S3). Therefore, for this particular amino acid, a change from Asn to Asp could cause a local conformational perturbation, which may manifest itself in chemical shift differences, especially if the side-chain amino group is involved in structurally relevant interactions. We also inspected the seven Asn residues and their local environments in the X-ray structure of wild-type γD-crystallin (PDB: 1HK0; Basak et al., 2003). N33 is unique because it is involved in an H-bonding network across the first Greek key in the NTD (Figure S5). The NH_2 group of the N33 side chain donates an H bond to the backbone carbonyl of E7, as well as to the side-chain carboxyl of D73. These interactions will no longer be possible in the Asn to Asp mutant and, as a result, chemical shift changes for E7 and D73 would be expected in the mutant spectrum. This is indeed the case. Further contacts are present between the backbone amide of N33 and the Y6 backbone carbonyl, H-bonding across a β sheet, as well as the N33 backbone carbonyl and the adjacent S34 side chain. It appears that, without the amino group, which links two structural elements on either side, the backbone conformation of the N33-S34 unit is affected. This is consistent with the S34 amide group exhibiting the largest chemical shift difference upon Asn to Asp mutation.

For the N124D mutant, we inspected the conformational details in our current X-ray structure of this variant and compared them with those in the X-ray structure of wild-type γD-crystallin (PDB: 1HK0; Basak et al., 2003). The two β sheet backbone H bonds between N/D124 and R90 are preserved in both structures (Figure S6), suggesting that no significant chemical shift changes of amide resonances will be caused. In contrast, in the D124 mutant structure, the H bond between the amino group of the N124 side chain and the backbone carbonyl of G148 that is seen in wild-type γD-crystallin (Figure S6) is no longer present.

We also compared the X-ray structures of the N160D variant and the wild-type γD-crystallin (PDB: 1HK0) in relation to the NMR results. The N160D mutant exhibited minimal amide chemical shift changes in the ^{1}H,^{15}N HSQC spectrum (Figure 2), with the exceptions of V163 and G164, whose amide resonances displayed composite chemical shift differences of 0.522 and 0.23 ppm, respectively. These residues are located in a loop close to the mutation site and adjacent to R162 in the X-ray structure, which can form a salt bridge with E134 in the N160D mutant (Figure S7). Again, the crystallographic details match the NMR data (Figure 3). The potential additional interaction seen in one of the

Please cite this article in press as: Guseman et al., Assessing the Structures and Interactions of γD-Crystallin Deamidation Variants, Structure (2020), https://doi.org/10.1016/j.str.2020.11.006

CellPress

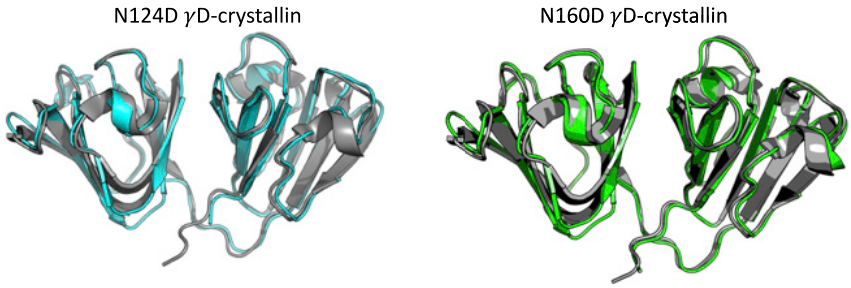

Figure 3. Structures of N124D (Cyan) and N160D (Green) γD-Crystallin Variants in Ribbon Representation, Superimposed on the Wild-Type Structure (PDB: 1HK0, gray).

two molecules in the N160D crystal structure may explain the 4.3°C increase in apparent T_m.

Interestingly, our results with respect to structure are similar to observations on congenital cataract variants of γD-crystallin, including three P23 variants, R76S, V75D, and W42R, as well as other mutants (McManus et al., 2007; Whitley et al., 2017; Ji et al., 2012, 2013a, 2013b). At position 23, P23S and P23V exhibit minimal structural changes (McManus et al., 2007) as does the P23T variant (Ji et al., 2013b). Finally, R76S, W42R, and V75D were also characterized by our group and none exhibited gross structural changes (Ji et al., 2012, 2013a; Whitley et al., 2017). Combining all these findings on the atomic structures of these variants and the current deamidated γD-crystallin variants reinforces the notion that γD-crystallin is robust in its ability to maintain its overall structure.

Given that only minimal structural differences were noted for the Asn to Asp mutants of γD-crystallin, the thermodynamic stability or reversible aggregation properties could have been significantly affected in the mutants. Such changes, however, were not observed, and only small thermal stability differences, all within ±5°C, were noted. These differences in an otherwise exceedingly stable protein are too small to be considered as a rationale for cataractogenesis. In addition, these results are contrary to data on Gln deamidation at positions 54 or 143, where Gln residues make key interdomain contacts and where the introduction of Glu results in destabilization of the protein (Flaugh et al., 2006). While our observed changes in structure and thermodynamic stability of γD-crystallin are minimal, deamidation in other crystallins can influence the protein's aggregation propensity, as shown for γS-crystallin, even if only minimal effects on structure and stability are seen (Brubaker et al., 2011). We, therefore, carefully investigated whether we could observe any such changes by analyzing DIP values that report on colloidal stability (Saluja et al., 2010; Lehermayr et al., 2011). No significant changes in DIP, a proxy for the second virial coefficient, was found. Therefore, the introduction of a negative charge by deamidation of any of the seven Asn residues in γD-crystallin variants does not significantly influence the self-interaction behavior of these molecules in solution.

Intriguingly, our results differ from those observed for γS-crystallin and β-crystallins, suggesting that not all crystallins are equally affected by deamidation. For example, deamidation does not change the structure of γS-crystallin but does alter its stability, aggregation propensity, and dynamics (Ray et al., 2016; Pande et al., 2015; Takemoto and Boyle, 2000; Forsythe et al., 2019; Vetter et al., 2020). For β-crystallins, deamidation can cause compaction, disrupt heterodimer formation, and promote formation of higher-order oligomers (Takata et al., 2008, 2010; Lampi et al., 2001, 2002, 2006, 2012, 2016; Michiel et al., 2010). Here, for γD-crystallin, no significant difference in stability or aggregation propensity was observed.

Overall, our data demonstrate that the aspartate product of Asn deamidation has minimal impact on the structure and biophysical properties of γD-crystallin. These results suggest that γD-crystallin can tolerate a single deamidation while maintaining its structure and function. However, we cannot exclude synergistic effects of additional deamidations or modifications, such

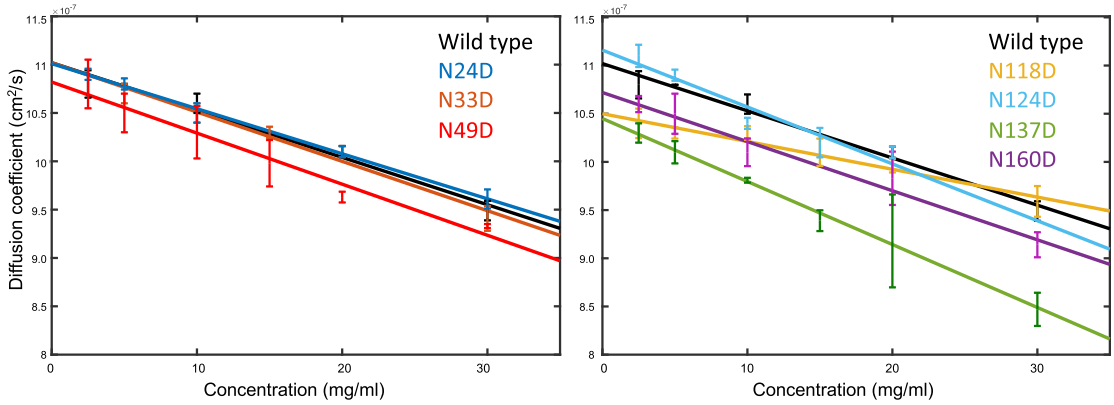

Figure 4. Concentration Dependence of the Diffusion Coefficient Determined by DLS for Wild-Type and Deamidation Variants of γD-Crystallin.

The diffusion interaction parameter for each variant can be calculated from the slope of the best-fit line.

Please cite this article in press as: Guseman et al., Assessing the Structures and Interactions of γD-Crystallin Deamidation Variants, Structure (2020), https://doi.org/10.1016/j.str.2020.11.006

Table 2. Melting Temperatures Determined by Differential Scanning Calorimetry

Variant	T_m (°C)
Wild-type	81.2
N24D	83.4
N33D	82.1
N49D	81.8
N118D	83.2
N124D	81.3
N137D	80.4
N160D	85.5

T_m, melting temperature.

Table 3. Diffusion Interaction Parameters Determined by Dynamic Light Scattering

Variant	DIP (mL/g)
Wild-type	−4 ± 1
N24D	−5 ± 1
N33D	−4.2 ± 0.5
N49D	−5 ± 1
N118D	−3 ± 1
N124D	−5 ± 2
N137D	−6 ± 1
N160D	−5 ± 2

DIP, diffusion interaction parameter.

as oxidation, on the structural or biophysical properties of the protein. To further elucidate the influences of deamidation or any modification, the lens environment has to be taken into account since the behavior of proteins in a crowded environment can be different from that in dilute solution, especially with respect to folding or protein-protein interactions (Guseman et al., 2018; Monteith et al., 2015).

Conclusions

Systematic biophysical analysis of γD-crystallin surface deamidation variants indicates that single Asn to Asp amino acid changes in γD-crystallin are unlikely to drive cataract formation. Both NMR and crystallographic data demonstrate that, at most, very minor conformational changes are induced, but these do not result in decreased protein stability or altered self-association behavior. Even if such changes are frequently observed in proteomic analyses of aged lenses, irrespective of whether they exhibit cataract (Hains and Truscott, 2010), our results serve as a cautionary tale for generally implicating deamidation from Asn to Asp in cataractogenesis. Whether any of the other intermediates or deamidation products in a particular α-, β-, or γ-crystallin contribute to, or cause, cataracts will require further detailed studies.

STAR★METHODS

Detailed methods are provided in the online version of this paper and include the following:

- KEY RESOURCES TABLE
- RESOURCE AVAILABILITY
  - Lead Contact
  - Material Availability
  - Data Availability
- EXPERIMENTAL MODEL AND SUBJECT DETAILS
  - Bacterial Cell Culture
- METHOD DETAILS
  - Expression and Purification
  - NMR Spectroscopy
  - Crystallization of γD-Crystallin Asp Variants
  - X-ray Diffraction and Structure Determination
  - Dynamic Light Scattering
  - Differential Scanning Calorimetry
- QUANTIFICATION AND STATISTICAL ANALYSIS

SUPPLEMENTAL INFORMATION

Supplemental Information can be found online at https://doi.org/10.1016/j.str.2020.11.006.

ACKNOWLEDGMENTS

Members of the Gronenborn laboratory are gratefully acknowledged for assistance and insightful comments, and George Makhatadze for discussions on differential scanning calorimetry. We thank Doug Bevan for computer, Mike Delk for NMR, and Doowon Lee for X-ray technical support, and Teresa Brosenitsch for critically reading the manuscript. This work was supported by NIH grants R01 EY030057. A.J.G. is a Merck fellow of the Life Sciences Research Foundation and holds a Postdoctoral Enrichment Program Award from the Burroughs Wellcome Fund.

AUTHOR CONTRIBUTIONS

A.J.G., M.J.W., and A.M.G. designed the experiments. A.J.G., M.J.W., J.J.G., N.R., and M.A. prepared the samples. M.J.W., N.R., and M.A. conducted crystallographic studies. A.J.G. and J.J.G. performed NMR and light scattering. A.J.G. performed DSC experiments. A.J.G., M.J.W., and A.M.G. wrote the manuscript and all authors reviewed and approved the manuscript.

DECLARATION OF INTERESTS

The authors declare no conflict of interest.

Received: June 14, 2020
Revised: October 12, 2020
Accepted: November 6, 2020
Published: December 1, 2020

REFERENCES

Adams, P.D., Afonine, P.V., Bunkoczi, G., Chen, V.B., Davis, I.W., Echols, N., Headd, J.J., Hung, L.-W., Kapral, G.J., Grosse-Kunstleve, R.W., et al. (2010). Phenix: a comprehensive python-based system for macromolecular structure solution. Acta Crystallogr. Sec. D *66*, 213–221.

Basak, A., Bateman, O., Slingsby, C., Pande, A., Asherie, N., Ogun, O., Benedek, G.B., and Pande, J. (2003). High-resolution X-ray crystal structures of human γD crystallin (1.25 Å) and the R58H mutant (1.15 Å) associated with aculeiform cataract. J. Mol. Biol. *328*, 1137–1147.

Bloemendal, H., De JONG, W., Jaenicke, R., Lubsen, N.H., Slingsby, C., and Tardieu, A. (2004). Ageing and vision: structure, stability and function of lens crystallins. Prog. Biophys. Mol. Biol. *86*, 407–485.

Boatz, J.C., Whitley, M.J., Li, M., Gronenborn, A.M., and Van Der Wel, P.C.A. (2017). Cataract-associated P23T γD-crystallin retains a native-like fold in amorphous-looking aggregates formed at physiological pH. Nat. Commun. *8*, 15137.

Please cite this article in press as: Guseman et al., Assessing the Structures and Interactions of γD-Crystallin Deamidation Variants, Structure (2020), https://doi.org/10.1016/j.str.2020.11.006

Brubaker, W.D., Freites, J.A., Golchert, K.J., Shapiro, R.A., Morikis, V., Tobias, D.J., and Martin, R.W. (2011). Separating instability from aggregation propensity in γS-crystallin variants. Biophys. J. *100*, 498–506.

Clarke, S. (1987). Propensity for spontaneous succinimide formation from aspartyl and asparaginyl residues in cellular proteins. Int. J. Pept. Protein Res. *30*, 808–821.

D'arcy, A., Villard, F., and Marsh, M. (2007). An automated microseed matrix-screening method for protein crystallization. Acta Crystallogr. Sec. D. *63*, 550–554.

Emsley, P., and Cowtan, K. (2004). Coot: model-building tools for molecular graphics. Acta Crystallogr. Sec. D *60*, 2126–2132.

Estrada, J., Bernadó, P., blackledge, M., and Sancho, J. (2009). ProtSA: a web application for calculating sequence specific protein solvent accessibilities in the unfolded ensemble. BMC Bioinformatics *10*, 104.

Flaugh, S.L., Mills, I.A., and King, J. (2006). Glutamine deamidation destabilizes human γD-crystallin and lowers the kinetic barrier to unfolding. J. Biol. Chem. *281*, 30782–30793.

Forman-Kay, J.D., Clore, G.M., Stahl, S.J., and Gronenborn, A.M. (1992). ^{1}H and ^{15}N resonance assignments and secondary structure of the human thioredoxin C62A, C69A, C73A mutant. J. Biomol. NMR *2*, 431–445.

Forsythe, H.M., Vetter, C.J., Jara, K.A., Reardon, P.N., David, L.L., Barbar, E.J., and Lampi, K.J. (2019). Altered protein dynamics and increased aggregation of human γS-crystallin due to cataract-associated deamidations. Biochemistry *58*, 4112–4124.

Geiger, T., and Clarke, S. (1987). Deamidation, isomerization, and racemization at asparaginyl and aspartyl residues in peptides. Succinimide-linked reactions that contribute to protein degradation. J. Biol. Chem. *262*, 785–794.

Ghosh, K.S., and Chauhan, P. (2019). Crystallins and their complexes. In Macromolecular Protein Complexes II: Structure and Function, J.R. Harris and J. Marles-Wright, eds. (Springer International Publishing), pp. 439–460.

Guseman, A.J., Speer, S.L., Perez Goncalves, G.M., and Pielak, G.J. (2018). Surface charge modulates protein-protein interactions in physiologically relevant environments. Biochemistry *57*, 1681–1684.

Hains, P.G., and Truscott, R.J.W. (2010). Age-dependent deamidation of lifelong proteins in the human lens. Invest. Ophthalmol. Vis. Sci. *51*, 3107–3114.

Hanson, S.R.A., Hasan, A., Smith, D.L., and Smith, J.B. (2000). The major in vivo modifications of the human water-insoluble lens crystallins are disulfide bonds, deamidation, methionine oxidation and backbone cleavage. Exp. Eye Res. *71*, 195–207.

Haslbeck, M., Peschek, J., Buchner, J., and Weinkauf, S. (2016). Structure and function of α-crystallins: traversing from in vitro to in vivo. Biochim. Biophys. Acta *1860*, 149–166.

Jaenicke, R., and Slingsby, C. (2001). Lens crystallins and their microbial homologs: structure, stability, and function. Crit. Rev. Biochem. Mol. Biol. *36*, 435–499.

Jehle, S., Rajagopal, P., Bardiaux, B., Markovic, S., Kühne, R., Stout, J.R., Higman, V.A., Klevit, R.E., Van Rossum, B.-J., and Oschkinat, H. (2010). Solid-state NMR and SAXS studies provide a structural basis for the activation of αB-crystallin oligomers. Nat. Struct. Mol. Biol. *17*, 1037–1042.

Ji, F., Jung, J., and Gronenborn, A.M. (2012). Structural and biochemical characterization of the childhood cataract-associated R76S mutant of human γD-crystallin. Biochemistry *51*, 2588–2596.

Ji, F., Jung, J., Koharudin, L.M.I., and Gronenborn, A.M. (2013a). The human W42R γD-crystallin mutant structure provides a link between congenital and age-related cataracts. J. Biol. Chem. *288*, 99–109.

Ji, F., Koharudin, L.M.I., Jung, J., and Gronenborn, A.M. (2013b). Crystal structure of the cataract-causing P23T γD-crystallin mutant. Proteins *81*, 1493–1498.

Kabsch, W. (2010). Xds. Acta Crystallogr. Sec. D *66*, 125–132.

Lam, D., Rao, S.K., Ratra, V., Liu, Y., Mitchell, P., King, J., Tassignon, M.-J., Jonas, J., Pang, C.P., and Chang, D.F. (2015). Cataract. Nat. Rev. Dis. *1*, 15014.

Lampi, K.J., Amyx, K.K., Ahmann, P., and Steel, E.A. (2006). Deamidation in human lens βB2-crystallin destabilizes the dimer. Biochemistry *45*, 3146–3153.

Lampi, K.J., Fox, C.B., and David, L.L. (2012). Changes in solvent accessibility of wild-type and deamidated βB2-crystallin following complex formation with αA-crystallin. Exp. Eye Res. *104*, 48–58.

Lampi, K.J., Kim, Y.H., Bächinger, H.P., Boswell, B.A., Lindner, R.A., Carver, J.A., Shearer, T.R., David, L.L., and Kapfer, D.M. (2002). Decreased heat stability and increased chaperone requirement of modified human betab1-crystallins. Mol. Vis. *8*, 359–366.

Lampi, K.J., Ma, Z., Hanson, S.R.A., Azuma, M., Shih, M., Shearer, T.R., Smith, D.L., Smith, J.B., and David, L.L. (1998). Age-related changes in human lens crystallins identified by two-dimensional electrophoresis and mass spectrometry. Exp. Eye Res. *67*, 31–43.

Lampi, K.J., Murray, M.R., Peterson, M.P., Eng, B.S., Yue, E., Clark, A.R., Barbar, E., and David, L.L. (2016). Differences in solution dynamics between lens β-crystallin homodimers and heterodimers probed by hydrogen-deuterium exchange and deamidation. Biochim. Biophys. Acta *1860*, 304–314.

Lampi, K.J., Oxford, J.T., Bachinger, H.P., Shearer, T.R., David, L.L., and Kapfer, D.M. (2001). Deamidation of human βB1 alters the elongated structure of the dimer. Exp. Eye Res. *72*, 279–288.

Lampi, K.J., Wilmarth, P.A., Murray, M.R., and David, L.L. (2014). Lens β-crystallins: the role of deamidation and related modifications in aging and cataract. Prog. Biophys. Mol. Biol. *115*, 21–31.

Lee, W., Tonelli, M., and Markley, J.L. (2014). NMRFAM-SPARKY: enhanced software for biomolecular NMR spectroscopy. Bioinformatics *31*, 1325–1327.

Lehermayr, C., Mahler, H.-C., Mäder, K., and Fischer, S. (2011). Assessment of net charge and protein-protein interactions of different monoclonal antibodies. J. Pharm. Sci. *100*, 2551–2562.

Liebschner, D., Afonine, P.V., Baker, M.L., Bunkoczi, G., Chen, V.B., Croll, T.I., Hintze, B., Hung, L.-W., Jain, S., Mccoy, A.J., et al. (2019). Macromolecular structure determination using X-rays, neutrons and electrons: recent developments in phenix. Acta Crystallogr. Sec. D *75*, 861–877.

Lynnerup, N., Kjeldsen, H., Heegaard, S., Jacobsen, C., and Heinemeier, J. (2008). Radiocarbon dating of the human eye lens crystallines reveal proteins without carbon turnover throughout life. PLoS One *3*, e1529.

Mccoy, A.J., Grosse-Kunstleve, R.W., Adams, P.D., Winn, M.D., Storoni, L.C., and Read, R.J. (2007). Phaser crystallographic software. J. Appl. Crystallogr. *40*, 658–674.

Mcmanus, J.J., Lomakin, A., Ogun, O., Pande, A., Basan, M., Pande, J., and Benedek, G.B. (2007). Altered phase diagram due to a single point mutation in human γD-crystallin. Proc. Natl. Acad. Sci. U S A *104*, 16856.

Michiel, M., Duprat, E., Skouri-Panet, F., Lampi, J.A., Tardieu, A., Lampi, K.J., and Finet, S. (2010). Aggregation of deamidated human βB2-crystallin and incomplete rescue by α-crystallin chaperone. Exp. Eye Res. *90*, 688–698.

Monteith, W.B., Cohen, R.D., Smith, A.E., Guzman-Cisneros, E., and Pielak, G.J. (2015). Quinary structure modulates protein stability in cells. Proc. Natl. Acad. Sci. U S A *112*, 1739.

Pande, A., Mokhor, N., and Pande, J. (2015). Deamidation of human γS-crystallin increases attractive protein interactions: implications for cataract. Biochemistry *54*, 4890–4899.

Ray, N.J., Hall, D., and Carver, J.A. (2016). Deamidation of N76 in human γS-crystallin promotes dimer formation. Biochim. Biophys. Acta *1860*, 315–324.

Robinson, N.E. (2002). Protein deamidation. Proc. Natl. Acad. Sci. U S A *99*, 5283.

Robinson, N.E., Lampi, K.J., Speir, J.P., Kruppa, G., Easterling, M., and Robinson, A.B. (2006). Quantitative measurement of young human eye lens crystallins by direct injection Fourier transform ion cyclotron resonance mass spectrometry. Mol. Vis. *12*, 704–711.

Saluja, A., Fesinmeyer, R.M., Hogan, S., Brems, D.N., and Gokarn, Y.R. (2010). Diffusion and sedimentation interaction parameters for measuring the second virial coefficient and their utility as predictors of protein aggregation. Biophys. J. *99*, 2657–2665.

Serebryany, E., Yu, S., Trauger, S.A., Budnik, B., and Shakhnovich, E.I. (2018). Dynamic disulfide exchange in a crystallin protein in the human eye lens promotes cataract-associated aggregation. J. Biol. Chem. *293*, 17997–18009.

Sharma, K.K., and Santhoshkumar, P. (2009). Lens aging: effects of crystallins. Biochim. Biophys. Acta *1790*, 1095–1108.

Srivastava, O.P., and Srivastava, K. (2003). Existence of deamidated αB-crystallin fragments in normal and cataractous human lenses. Mol. Vis. *9*, 110–118.

Takata, T., Oxford, J.T., Demeler, B., and Lampi, K.J. (2008). Deamidation destabilizes and triggers aggregation of a lens protein, βA3-crystallin. Protein Sci. *17*, 1565–1575.

Takata, T., Smith, J.P., Arbogast, B., David, L.L., and Lampi, K.J. (2010). Solvent accessibility of βB2-crystallin and local structural changes due to deamidation at the dimer interface. Exp. Eye Res. *91*, 336–346.

Takemoto, L., and Boyle, D. (2000). Increased deamidation of asparagine during human senile cataractogenesis. Mol. Vis. *6*, 164–168.

Terwilliger, T.C., Grosse-Kunstleve, R.W., Afonine, P.V., Moriarty, N.W., Zwart, P.H., Hung, L.-W., Read, R.J., and Adams, P.D. (2008). Iterative model building, structure refinement and density modification with the Phenix autobuild wizard. Acta Crystallogr. Sec. D *64*, 61–69.

Toyama, B.H., and Hetzer, M.W. (2012). Protein homeostasis: live long, won't prosper. Nat. Rev. Mol. Cell. Biol. *14*, 55.

Vetter, C.J., Thorn, D.C., Wheeler, S.G., Mundorff, C., Halverson, K., Wales, T.E., Shinde, U., Engen, J.R., David, L.L., Carver, J.A., and Lampi, K.J. (2020). Cumulative deamidations of the major lens protein γS-crystallin increase its aggregation during unfolding and oxidation. Protein Sci. *29*, 1945–1963.

Wang, J., Zuo, X., Yu, P., Byeon, I.-J.L., Jung, J., Wang, X., Dyba, M., Seifert, S., Schwieters, C.D., Qin, J., et al. (2009). Determination of multicomponent protein structures in solution using global orientation and shape restraints. J. Am. Chem. Soc. *131*, 10507–10515.

Warmack, R.A., Shawa, H., Liu, K., Lopez, K., Loo, J.A., Horwitz, J., and Clarke, S.G. (2019). The L-isoaspartate modification within protein fragments in the aging lens can promote protein aggregation. J. Biol. Chem. *294*, 12203–12219.

Whitley, M.J., Xi, Z., Bartko, J.C., Jensen, M.R., Blackledge, M., and Gronenborn, A.M. (2017). A combined NMR and SAXS analysis of the partially folded cataract-associated V75D γD-crystallin. Biophys. J. *112*, 1135–1146.

Williamson, M.P. (2013). Using chemical shift perturbation to characterise ligand binding. Prog. Nucl. Magn. Reson. Spectrosc. *73*, 1–16.

Wilmarth, P.A., Tanner, S., Dasari, S., Nagalla, S.R., Riviere, M.A., Bafna, V., Pevzner, P.A., and David, L.L. (2006). Age-related changes in human crystallins determined from comparative analysis of post-translational modifications in young and aged lens: does deamidation contribute to crystallin insolubility? J. Proteome Res. *5*, 2554–2566.

Zhao, H., Brown, P.H., Magone, M.T., and Schuck, P. (2011a). The molecular refractive function of lens γ-crystallins. J. Mol. Biol. *411*, 680–699.

Zhao, H., Magone, M.T., and Schuck, P. (2011b). The role of macromolecular crowding in the evolution of lens crystallins with high molecular refractive index. Phys. Biol. *8*, 046004.

Please cite this article in press as: Guseman et al., Assessing the Structures and Interactions of γD-Crystallin Deamidation Variants, Structure (2020), https://doi.org/10.1016/j.str.2020.11.006

STAR★METHODS

KEY RESOURCES TABLE

REAGENT or RESOURCE	SOURCE	IDENTIFIER
Bacterial and Virus Strains		
Escherichia coli BL21(DE3)	NEB	Cat# C2527H
Chemicals, Peptides, and Recombinant Proteins		
Tris	Fisher	Cat# 61202-5000
MES	Sigma	Cat#5287
EDTA	Fisher	Cat#AAJ15694AE
TCEP	Sigma	Cat#C4706
DTT	RPI	Cat#D11000
NaCl	Sigma	Cat#S7653
^{15}N NH_4Cl	Cambridge isotope labs	Cat#NLM-467
D_2O	Cambridge isotope labs	Cat#DLM-4
IPTG	RPI	Cat#I56000
Deposited Data		
Crystal structure of γD-crystallin	Basek et al., 2003	PDB: 1HK0
NMR Structure of γD-crystallin	Wang et al., 2009	PDB: 2KLJ
Crystal structure of N124D γD-crystallin	This paper	PDB: 6W5B
Crystral structure of N160D γD- crystallin	This paper	PDB: 6WCY
Recombinant DNA		
pET14b CRYGD	Ji et al., 2012	N/A
Modified pET14b vectors	This paper	N/A
Software and Algorithms		
NMRFAM-SPARKY	Lee et al., 2014	https://nmrfam.wisc.edu/nmrfam-sparky-distribution/
Phaser	McCoy et al., 2007	https://www.ccp4.ac.uk
COOT	Emsley and Cowtan, 2004	https://www2.mrc-lmb.cam.ac.uk/personal/pemsley/coot/
Phenix AutoBuild	Terwilliger et al., 2008	https://www.phenix-online.org/documentation/reference/autobuild.html
Origin	Malvern	N/A
Phenix	Adams et al., 2010	https://www.phenix-online.org
PyMol	Schrödinger	https://pymol.org/2/
protSA	Estrada et al., 2009	http://webapps.bifi.es/ProtSA/
Matlab	Mathworks	N/A
Dynamics 7.1.7	Wyatt Technologies	N/A
Other		
384-well DLS plate	Corning	Cat#3540
HiTrap Q HP	GE Healthcare	Cat#17115401
HiTrap HP SP	GE Healthcare	Cat# 17115201
Amicon Spin Concentator 10000 MWCO	Amicon	Cat# UFC901024
HiLoad 16/600 Superdex 75 pg	GE Healthcare	Cat#28989333

RESOURCE AVAILABILITY

Lead Contact

Further information and reagent requests should be addressed to lead contact Angela Gronenborn (amg100@pitt.edu).

Material Availability

This study did not generate new unique reagents.

Data Availability

Atomic coordinates for the N124D and N160D γD-crystallin variants are deposited in the RCSB PDB with accession codes 6W5B and 6WCY, respectively.

EXPERIMENTAL MODEL AND SUBJECT DETAILS

Bacterial Cell Culture

BL21(DE3) cells obtained from New England BioLabs (cat #C2527H) were used for expression of human γD-crystallin and Asp variants. Cells harboring the transformed γD-crystallin plasmid were cultured in LB broth or modified M9 minimal medium with 100 μg/ml of carbenicillin at 37°C.

METHOD DETAILS

Expression and Purification

Human γD-crystallin and the Asp variants were expressed and purified as previously described (Ji et al., 2012). In short, BL21(DE3) *E. coli* cells were transformed with a pET14b vector containing either the WT *CRYGD* gene or a deamidation variant. Cells harboring the transformed γD-crystallin plasmid were cultured in LB broth or modified M9 minimal medium containing 1 g/L $^{15}NH_4Cl$ and grown to an absorbance (A_{600}) between 0.6-0.8, at which time 1 mM IPTG was added, and protein expression was continued for 4 hours. Cells were harvested by centrifugation and resuspended in Q_a buffer (20 mM Tris pH 8.0, 1mM EDTA, 1 mM DTT). Cells were lysed by microfluidization, lysates were cleared by centrifugation at 39,000*g* for 40 minutes, and the supernatant was collected and filtered through a 0.22 μm filter. The cleared supernatant was passed over a HiTrap Q HP anion exchange column pre-equilibrated at 4°C, and the flow through was collected and dialyzed overnight into 4 L of S_a buffer (20 mM MES pH 6.0, 1mM EDTA, 1 mM DTT). Post dialysis, aggregates were removed by centrifugation at 39,000*g* for 20 minutes, and the supernatant was passed through a 0.22 μm filter and loaded on a HiTrap HP SP cation exchange column in S_a buffer. Protein was eluted using a linear gradient of 0-50% S_b (20 mM MES pH 6.0, 1mM EDTA, 1 mM DTT, 1 M NaCl) over 10 column volumes. 5 mL fractions were collected, and fractions that contained γD-crystallin were pooled and concentrated to <5 mL using an Amicon spin concentrator. The final purification involved gel filtration over an S75 16/600 column in S_a buffer. Fractions were analyzed by SDS PAGE, and those containing pure γD-crystallin were collected, pooled, and concentrated to less than 2 mL total volume. Protein concentration was determined using a Nanodrop ND-1000 and a molar extinction coefficient of 40680 M^{-1} cm^{-1}.

NMR Spectroscopy

All NMR experiments were carried out at 25°C using a Bruker AVANCE 800 MHz spectrometer equipped with a z-axis gradient, triple resonance cryoprobe. 2D ^{1}H-^{15}N HSQC spectra were recorded on samples containing 150 μM protein in 20 mM MES buffer, 1 mM EDTA, 1 mM TCEP, pH 6.0 and 10% D_2O. Resonance assignments were carried out in NMRFAM-SPARKY (Lee et al., 2014) and crosschecked against previously published assignments for the wild-type protein (Ji et al., 2012). Chemical shift differences for the mutant variants were calculated according to

$$\Delta\delta : \sqrt{(\delta_{H_v} - \delta_{H_{wt}})^2 + \left(\frac{\delta_{N_v} - \delta_{N_{wt}}}{6}\right)^2}$$

(Williamson, 2013).

Crystallization of γD-Crystallin Asp Variants

The N124D and N160D deamidation mutants were concentrated to 10 mg/mL in size exclusion buffer. Crystallization trials were performed using sitting drop vapor diffusion. An initial crystallization hit with N124D was obtained in 0.2 M magnesium chloride hexahydrate, 0.1 M Tris (pH 7.0), and 10% w/v PEG 8000; these crystals were crushed and diluted in the same solution to serve as a seed stock for random matrix microseeding (rMMS) trials (D'Arcy et al., 2007). Diffraction quality crystals were obtained in a crystallization solution consisting of 0.2 M lithium sulfate, 0.1 M phosphate-citrate (pH 4.2), and 20% w/v PEG 1000. Crystals were harvested, vitrified in liquid nitrogen without additional cryoprotection and used for data collection. For N160D, initial poor-quality plate-type crystals were obtained in 25% w/v PEG 3350, 0.1 M Bis-Tris (pH 5.5), and 0.2 M ammonium sulfate. Crushed crystals were used for rMMS, which yielded numerous crystals of high quality. Final crystals, grown in 0.1 M succinic acid (pH 7.0) and 15% w/v PEG 3350, were harvested, vitrified in liquid nitrogen without additional cryoprotectant, and used for data collection.

X-ray Diffraction and Structure Determination

Diffraction data for N124D were recorded at the GM/CA beamline 23-ID-D of the Advanced Photon Source at Argonne National Laboratory (Lemont, IL, USA). The X-ray wavelength was 0.8856 Å, and 1800 images were recorded at an oscillation width of 0.2° per image. Diffraction data for N160D were recorded at SER-CAT beamline 22-ID of the Advanced Photon Source at Argonne National Laboratory. Using X-rays of wavelength 1.0 Å, 720 diffraction images were recorded at an oscillation width of 0.5° per image. Data

Please cite this article in press as: Guseman et al., Assessing the Structures and Interactions of γD-Crystallin Deamidation Variants, Structure (2020), https://doi.org/10.1016/j.str.2020.11.006

reduction and scaling were performed with XDS (Kabsch, 2010). N124D crystallized in the primitive orthorhombic space group $P2_12_12_1$ with a single molecule in the asymmetric unit. N160D also crystallized in space group $P2_12_12_1$, but with two molecules in the asymmetric unit. For each mutant, phases were determined by molecular replacement in Phaser (McCoy et al., 2007), using the WT structure (PDB 1HK0) as the search model. Before molecular replacement, the four tryptophan side chains in the search model were truncated to alanine, and the presence of side chain density for these tryptophans in the molecular replacement solutions was used to validate their correctness. The molecular replacement solutions were rebuilt using Phenix AutoBuild (Terwilliger et al., 2008) and subjected to multiple iterations of manual model correction in Coot (Emsley and Cowtan, 2004) and automated refinement in Phenix (Liebschner et al., 2019; Adams et al., 2010). Riding hydrogens were added to both mutant models for refinement. Anisotropic atomic displacement parameters (ADP) were refined for N124D. For N160D, refinement of anisotropic ADP led to a large decrease in R_{work} but a much smaller decrease in R_{free}. To avoid overfitting, refinement of anisotropic ADP was abandoned for this mutant in favor of a simpler TLS model, which led to a similar decrease in both R_{work} and R_{free}. Non-crystallographic symmetry restraints were also used during N160D refinement. Final refinement for the N124D and N160D models was to a resolution of 1.15 and 1.20 Å, respectively. Full data collection and refinement statistics are provided in Table 1. The diffraction data and refined models for N124D and N160D γD-crystallin were deposited in the Protein Data Bank under accession codes 6W5B and 6WCY, respectively.

Dynamic Light Scattering

Purified human γD-crystallin was concentrated to >50 mg/mL in 20 mM MES buffer, 1mM EDTA, 1 mM DTT, pH 6.0. Buffer and protein solutions were filtered through a 0.01 μm filter, and concentrations were determined spectroscopically, using an extinction coefficient of 40680 M^{-1} cm^{-1}. DLS was performed using a DynaPro Plate Reader III (Wyatt Technology, Santa Barbara, CA) in a 384 well plate format at 298 K. Samples (60 μL) at protein concentrations between 2.5 and 30 mg/mL were prepared, and triplicates of 20 μL each were measured. Ten acquisitions were collected for each sample, and data for the ten acquisitions were averaged. Data were analyzed in Dynamics 7.1.7, plotted in MatLab and fit to $D = (D_0 + D_0 k_D c)$, with D the diffusion coefficient, D_0 the diffusion coefficient at infinite dilution, k_D the diffusion interaction parameter, and c the protein concentration, uncertainties reflect the 95% confidence interval of the fit and are reported in Table 3.

Differential Scanning Calorimetry

Thermal unfolding was performed on a Microcal VP-DSC microcalorimeter. Crystallin variants were dialyzed twice against five liters of water. The dialysis water was filtered and saved for recording the reference baseline. The temperature was ramped from 25-110°C per scan at 90°C/hour. The data were analyzed using the Origin DSC software package.

QUANTIFICATION AND STATISTICAL ANALYSIS

Details of statistical analysis can be found in the methods description for each technique used. In Short, DLS data was analyzed in Dynamics 7.1.7 and plotted in MatLab which was also used to fit the data as described in the STAR Methods section, the uncertainties reflect the 95% confidence interval of the fit and is reported in Table 3. DSC thermograms were analyzed in Origin DSC software package to determine T_m and are reported in Table 2. Finally, a detailed description of the statistics for the X-ray structure determination are stated in the STAR Methods section and reported in Table 1.